Low Complexity OTFS Detection with a Delay-Doppler Domain CMC-MMSE Receiver

Yanjun Pan*, *Member, IEEE*, Jingxian Wu,* *Senior Member, IEEE*, and Jinhong Yuan,† *Fellow, IEEE*

***Abstract*—A low complexity receiver is developed for orthogonal time frequency space (OTFS) systems by exploring the special structure of the delay-Doppler (DD) domain channel matrix. Based on the system architecture of OTFS, we propose to shuffle the received samples in the DD domain such that samples experiencing the same delay but different Doppler spreads are grouped together. It is shown through theoretical analysis that the proposed shuffling operation yields a special block-circulant-like structure of the DD domain channel matrix. Enabled by the special structure, we propose to develop an iterative receiver that performs coherent matrix combining (CMC) with minimum mean squared error (MMSE) detection in the DD domain. The proposed receiver can collect the diversity in both the delay and Doppler domains while simultaneously suppress the negative impacts of DD domain intersymbol interference (ICI). Simulation results show that the proposed DD-CMC-MMSE receiver achieves significant performance gain over the commonly used message passing (MP) receiver for OTFS systems.**

I. Introduction

Orthogonal time frequency space (OTFS) is a promising modulation scheme that can provide reliable and efficient wireless communications in high mobility scenarios [1], [2]. OTFS modulates the signal in the delay-Doppler (DD) domain, which changes much slower than the conventional time-frequency domain with time and frequency doubly-selective channel. It is shown in [3] that OTFS is insensitive to Doppler spread while the performance of orthogonal frequency division multiplexing (OFDM) degrades significantly under high mobility scenarios.

One of the main challenges faced by the development of OTFS systems is the design of low complexity detectors. Various detection methods have been proposed in the literature to balance the tradeoff between detection performance and complexity. In [4], an iterative parallel interference cancellation (PIC) scheme is proposed to mitigate the impacts of intersymbol interference (ICI) in the DD domain, and the first iteration is initialized by using a minimum mean squared error (MMSE) equalization in the time-frequency domain. An iterative receiver with time domain MMSE is proposed in [5] for zero-padding OTFS (ZP-OTFS), where zeros are padded at the end of an OTFS frame to reduce interference. In [6], a message passing (MP) algorithm utilizing DD channel sparsity was proposed for joint interference cancellation and symbol detection. An approximate message passing (AMP) based detector was designed in [7] to handle a large number of channel paths or fractional Doppler shifts. In [8], an iterative rake decision feedback detector is proposed, and it extracts and coherently combines received multipath components of transmitted symbols on the delay-Doppler grid using maximal ratio combining (MRC). A cross domain iterative detection approach is introduced in [9], where the receiver employs basic estimation techniques in both the time domain and the DD domain and iteratively updates the extrinsic information from these two domains using unitary transformations.

In this paper, we develop a low complexity receiver for OTFS systems by exploring the special structure of the DD domain channel matrix. Based on the system architecture of OTFS in both the time-frequency and delay-Doppler domains, we propose to shuffle the DD domain samples at the receiver, such that samples experiencing the same delay but different Doppler spreads are grouped together. It is shown through theoretical analysis that the proposed shuffling operation leads to a block-circulant-like structure of the DD domain channel matrix. The structure of the DD domain channel matrix indicates that an information symbol transmitted over a single delay-Doppler point at the transmitter has been spread over multiple delays and Doppler spreads due to the effects of the doubly-selective fading channel.

We propose to exploit the delay-Doppler signal dispersion with a new iterative receiver in the DD domain. In each iteration, the receiver first performs coherent matrix combining (CMC) over multiple copies of the same symbol with different delays to collect the delay diversity. The coherent combining of the desired signal also results in the non-coherent combining of the interference symbols, thus achieves simultaneous diversity collection and interference suppression in the delay domain. Next an minimum mean squared error (MMSE) detector is used to collect the diversity and mitigate the impacts of ICI and noise in the Doppler domain. Successive interference cancellation (SIC) is performed to further improve system performance. Simulation results demonstrated that the newly proposed DD-CMC-MMSE receiver achieves significant performance gains over the commonly used MP receiver.

II. System Model

The system model of the OTFS systems is presented in this section. In the time-frequency domain, each OTFS frame contains N time symbols with symbol interval T, and M subcarriers with subcarrier spacing $\Delta f = \frac{1}{T}$. Consequently, the time interval between two consecutive OTFS frames in the time domain is NT, and the frequency spacing between two adjacent OTFS frames in the frequency domain is $M\Delta f$.

*Y. Pan and J. Wu are with the Department of Electrical Engineering and Computer Science, University of Arkansas, Fayetteville, AR 72701. †J. Yuan is with the School of Electrical Engineering and Telecommunications, University of New South Wales, Australia.

The delay-Doppler domain is discretized into an $N \times M$ grid with N levels in the Doppler domain and M levels in the delay domain. The resolutions in the delay and Doppler domains are determined by the time duration and frequency range of the OTFS frame in the time-frequency domain. The minimum delay domain interval is $\Delta\tau = \frac{1}{M\Delta f}$, and the minimum Doppler domain spacing is $\Delta\nu = \frac{1}{NT}$. Denote $x^{\text{DD}}[l,k]$ as the information symbol transmitted at delay $l\Delta\tau$ and Doppler shift $k\Delta\nu$, for $l = 0, \cdots, M-1$ and $k = 0, \cdots, N-1$.

At the transmitter, the delay-Doppler domain symbols are converted to the time-frequency domain by using inverse Symplectic finite Fourier transform (ISFFT) as

$$x^{\text{TF}}[m,n] = \frac{1}{\sqrt{MN}} \sum_{l=0}^{M-1} \sum_{k=0}^{N-1} x^{\text{DD}}[l,k] e^{j2\pi\left(\frac{nk}{N} - \frac{ml}{M}\right)}, \quad (1)$$

where $x^{\text{TF}}[m,n]$ is the time-frequency sample to be transmitted at subcarrier $m\Delta f$ and time nT.

The ISFFT in (1) can be written in a matrix format as

$$\mathbf{X}^{\text{TF}} = \mathbf{F}_M \cdot \mathbf{X}^{\text{DD}} \cdot \mathbf{F}_N^H, \quad (2)$$

where $\mathbf{F}_N$ is a size $N \times N$ discrete Fourier transform (DFT) matrix with the (k,l)-th element being $\frac{1}{\sqrt{N}} e^{-j\frac{2\pi kl}{N}}$, for $k,l = 0, \cdots, N-1$, $\mathbf{X}^{\text{TF}}$ and $\mathbf{X}^{\text{DD}}$ are $M \times N$ matrices with the (m,n)-th elelement being $x^{\text{TF}}[m,n]$ and $x^{\text{DD}}[m,n]$, respectively.

The discrete time-frequency samples are converted to discrete time domain samples by performing M-point IDFT as

$$s[k,n] = \frac{1}{\sqrt{M}} \sum_{m=0}^{M-1} x^{\text{TF}}[m,n] e^{j2\pi\frac{mk}{M}}, \quad \text{for} \quad k = 0,1,\cdots,M-1, n = 0,1,\cdots,N-1. \quad (3)$$

The discrete time samples cannot be directly transmitted in the wireless channel. They have to be pulse shaped before transmission. Denote the transmission pulse employed at the IDFT-based OTFS system as $q_{\text{TX}}(t)$ with bandwidth proportional to $\frac{1}{T_s} = \frac{M}{T}$, then the continuous-time transmitted signal can be represented as

$$s(t) = \sum_{n=0}^{N-1} \sum_{k=0}^{M-1} s[k,n] q_{\text{TX}}(t - nT - kT_s), \quad (4)$$

where $T_s = \frac{T}{M}$ is the duration of time-domain samples, and $T = MT_s$ is the duration of one IDFT block.

The continuous-time signal is transmitted through a doubly-selective channel with the DD domain channel impulse response as

$$\varphi(\tau,\nu) = \sum_{i=1}^{P} \varphi_i \delta(\tau - \tau_i)\delta(\nu - \nu_i), \quad (5)$$

where $\delta(\cdot)$ is the Dirac delta function, φ_i, τ_i, and ν_i are the path gain, delay, and Doppler shift for the i-th path, respectively, and P is the number of propagation paths. The signal observed at the receiver is

$$r(t) = \sum_{i=1}^{P} \varphi_i s(t - \tau_i) e^{j2\pi\nu_i(t-\tau_i)} + z(t), \quad (6)$$

where $z(t)$ is additive white Gaussian noise (AWGN) with one-sided power spectral density N_0.

The received signal passes through a matched filter $q_{\text{RX}}(t) = q_{\text{TX}}^*(-t)$. The signal at the output of the matched filter, $\eta(t) = r(t) \otimes q_{\text{TX}}^*(-t)$, can be represented as

$$\begin{aligned}\eta(t) &= \sum_{i=1}^{P} \varphi_i \int q_{\text{TX}}^*(t'-t) s(t'-\tau_i) e^{j2\pi\nu_i(t'-\tau_i)} dt' + w(t), \\ &= \sum_{n=0}^{N-1} \sum_{k=0}^{M-1} \sum_{i=1}^{P} \varphi_i s[k,n] e^{j2\pi\nu_i(nT+kT_s)} \\ &\quad A_{q_{\text{TX}}}(t - \tau_i - nT - kT_s, \nu_i) + w(t), \end{aligned} \quad (7)$$

where $w(t) = \int_{-\infty}^{\infty} q_{\text{TX}}^*(t'-t) z(t') dt'$ is the noise components at the output of the matched filter, and $A_{q_{\text{TX}}}(t,f)$ is the ambiguity function of $q_{\text{TX}}(t)$ defined as

$$A_{p_{\text{TX}}}(t,f) = \int_{-\infty}^{\infty} p_{\text{TX}}^*(\tau - t) p_{\text{TX}}(\tau) e^{j2\pi f\tau} d\tau. \quad (8)$$

The output of the matched filter is sampled at a sampling period T_s. The time domain samples corresponding to the n-th IDFT block at the transmitter, $\eta[k,n] = \eta(nT + kT_s)$, for $k = 0, \cdots, M-1$, can be represented as

$$\begin{aligned}\eta[k,n] = &\sum_{n'=0}^{N-1} \sum_{k'=0}^{M-1} s[k',n'] \times \\ &h_{nM+k}[(nM+k) - (n'M+k')] + w[k,n], \end{aligned} \quad (9)$$

where $h_k[k']$ is the equivalent time-varying impulse response defined as

$$h_k[l] = \sum_{i=1}^{P} \varphi_i e^{j2\pi\nu_i(k-l)T_s} A_{q_{\text{TX}}}(lT_s - \tau_i, \nu_i). \quad (10)$$

For a system that employs the rectangular waveform as $q_{\text{TX}}(t)$ with a duration T_s second, the closed-form expression of the ambiguity function $A_{q_{\text{TX}}(t)}$ can be found in [10, eqn. (26)]. The ambiguity function has a finite support in the time domain between $[-T_s, T_s]$. From (10), the range of l for $|h_k[l]| > 0$ can be calculated as $-T_s \le lT_s - \tau_{\max} \le T_s$, where $\tau_{\max} = \max(\tau_i)$ is the maximum delay spread of the physical channel. Thus the range of l is $0 \le l \le 1 + \lfloor \frac{\tau_{\max}}{T_s} \rfloor$. Consequently, the channel length is $L+1 = 2 + \lfloor \frac{\tau_{\max}}{T_s} \rfloor$, and the CP length for the IDFT implementation with the rectangular pulse-shaping waveform should be

$$L = 1 + \lfloor \frac{\tau_{\max}}{T_s} \rfloor. \quad (11)$$

After removal of CP at the receiver, the time-domain samples, $\{\eta[k,n]\}_{k=0,}^{M-1}$, can be converted to the time-frequency domain by using the M-point DFT as

$$y^{\text{TF}}[m,n] = \frac{1}{\sqrt{M}} \sum_{k=0}^{M-1} \eta[k,n] e^{-j2\pi\frac{mk}{M}}, m = 0,1,\cdots,M-1. \quad (12)$$

The time-frequency domain sample $y^{\text{TF}}[m,n]$ can be converted to the delay-Doppler domain by using SFFT, which can be written in a matrix format as

$$\mathbf{Y}^{\text{DD}} = \mathbf{F}_M^H \cdot \mathbf{Y}^{\text{TF}} \cdot \mathbf{F}_N, \text{ or } \quad \mathbf{Y}^{\text{TF}} = \mathbf{F}_M \cdot \mathbf{Y}^{\text{DD}} \cdot \mathbf{F}_N^H, \quad (13)$$

where $\mathbf{Y}^{\text{TF}}$ and $\mathbf{Y}^{\text{DD}}$ are an $M \times N$ matrices with the (m,n)-th element being $y^{\text{TF}}[m,n]$ and $y^{\text{DD}}[l,k]$, respectively, with $y^{\text{DD}}[l,k]$ being the received sample at delay $l\Delta\tau$ and Doppler shift $k\Delta v$, for $l = 0, \cdots, M-1$ and $k = 0, \cdots, N-1$.

III. System Architecture in the DD Domain

We propose to study the unique structure of the OTFS system in the DD domain, and the results will be used to design the low complexity receiver.

A. Matrix Representation

To facilitate the DD domain analysis, we first present the matrix representations of the OTFS system model. The time-domain OTFS system equation given in (9) can be represented in a matrix format as

$$\boldsymbol{\eta} = \mathbf{H}\mathbf{s} + \mathbf{w}, \tag{14}$$

where $\mathbf{H}$ is a $MN \times MN$ matrix defined in (16) at the top of the next page. The vectors $\boldsymbol{\eta}$, $\mathbf{s}$ and $\mathbf{w}$ are defined as

$$\boldsymbol{\eta} = \begin{bmatrix} \boldsymbol{\eta}_1 \\ \boldsymbol{\eta}_2 \\ \vdots \\ \boldsymbol{\eta}_N \end{bmatrix}, \quad \mathbf{s} = \begin{bmatrix} \mathbf{s}_1 \\ \mathbf{s}_2 \\ \vdots \\ \mathbf{s}_N \end{bmatrix}, \quad \mathbf{w} = \begin{bmatrix} \mathbf{w}_1 \\ \mathbf{w}_2 \\ \vdots \\ \mathbf{w}_N \end{bmatrix}, \tag{15}$$

where $\boldsymbol{\eta}_n$, $\mathbf{s}_n$, and $\mathbf{w}_n$ are size-M vectors with the $(k+1)$-th element being $y[k,n]$, $s[k,n]$, and $w[k,n]$, respectively, for $k = 0, \cdots, M-1$.

Applying M-point DFT to $\boldsymbol{\eta}_n$ yields the time-frequency sample vector $\mathbf{y}_n^{\text{TF}} = \mathbf{F}_M \boldsymbol{\eta}_n$. The corresponding time-frequency domain representation of the received signal is

$$\text{vec}\left(\mathbf{Y}^{\text{TF}}\right) = \mathbf{H}^{\text{TF}} \text{vec}\left(\mathbf{X}^{\text{TF}}\right) + \text{vec}\left(\mathbf{Z}^{\text{TF}}\right), \tag{17}$$

where $\mathbf{Y}^{\text{TF}} = [\mathbf{y}_1^{\text{TF}}, \cdots, \mathbf{y}_N^{\text{TF}}]$, $\mathbf{X}^{\text{TF}} = [\mathbf{x}_1^{\text{TF}}, \cdots, \mathbf{x}_N^{\text{TF}}]$, and $\mathbf{Z}^{\text{TF}} = [\mathbf{z}_1^{\text{TF}}, \cdots, \mathbf{z}_N^{\text{TF}}]$ are $M \times N$ matrices, with $\mathbf{x}_n^{\text{TF}} = \mathbf{F}_M \mathbf{s}_n$ and $\mathbf{z}_n^{\text{TF}} = \mathbf{F}_M \mathbf{w}_n$. The matrix $\mathbf{H}^{\text{TF}}$ is the equivalent time-frequency spread function matrix calculated as

$$\mathbf{H}^{\text{TF}} = \left(\mathbf{I}_N \otimes \mathbf{F}_M\right) \mathbf{H} \left(\mathbf{I}_N \otimes \mathbf{F}_M\right)^H. \tag{18}$$

With ISFFT in (2) and and SFFT in (13), we can rewrite the system equation in (17) as

$$\begin{aligned} \text{vec}\left(\mathbf{F}_M \mathbf{Y}^{\text{DD}} \mathbf{F}_N^H\right) =& \mathbf{H}^{\text{TF}} \cdot \text{vec}\left(\mathbf{F}_M \mathbf{X}^{\text{DD}} \mathbf{F}_N^H\right) + \\ & \text{vec}\left(\mathbf{F}_M \mathbf{Z}^{\text{DD}} \mathbf{F}_N^H\right), \end{aligned} \tag{19}$$

where $\mathbf{Z}^{\text{DD}} = \mathbf{F}_M^H \cdot \mathbf{Z}^{\text{TF}} \cdot \mathbf{F}_N$ is the DD domain noise matrix.

Based on the identity $\text{vec}\left(\mathbf{AXB}\right) = \left(\mathbf{B}^T \otimes \mathbf{A}\right) \cdot \text{vec}\left(\mathbf{X}\right)$ [11, eqn. (520)], where $\otimes$ represents matrix Kronecker product, the delay-Doppler domain system equation of the OTFS system can be written in a matrix format as

$$\text{vec}\left(\mathbf{Y}^{\text{DD}}\right) = \mathbf{H}^{\text{DD}} \cdot \text{vec}\left(\mathbf{X}^{\text{DD}}\right) + \text{vec}\left(\mathbf{Z}^{\text{DD}}\right), \tag{20}$$

where $\mathbf{H}^{\text{DD}} \in \mathcal{C}^{NM \times NM}$ is the equivalent delay-Doppler domain channel matrix. It can be calculated by using the time-frequency domain channel matrix as

$$\mathbf{H}^{\text{DD}} = \mathcal{F}^H \cdot \mathbf{H}^{\text{TF}} \cdot \mathcal{F}, \tag{21}$$

where $\mathcal{F} = \mathbf{F}_N^H \otimes \mathbf{F}_M$ is an orthonormal matrix.

Combining (18) and (21) yields

$$\mathbf{H}^{\text{DD}} = \left(\mathbf{F}_N \otimes \mathbf{I}_M\right) \cdot \mathbf{H} \cdot \left(\mathbf{F}_N \otimes \mathbf{I}_M\right)^H, \tag{22}$$

where the identity $\mathcal{F}^H(\mathbf{I}_N \otimes \mathbf{F}_M) = (\mathbf{F}_N \otimes \mathbf{F}_M^H)(\mathbf{I}_N \otimes \mathbf{F}_M) = \mathbf{F}_N \otimes \mathbf{I}_M$ is used in the above equation.

B. DD Domain Channel Structure

The DD domain channel matrix has special structures that can be utilized to simplify the receiver design. In order to reveal the special structure, we propose to shuffle the elements in $\mathbf{H}^{\text{DD}}$ as follows

$$\tilde{\mathbf{H}}^{\text{DD}} = \boldsymbol{\Gamma}_{MN}^T \mathbf{H}^{\text{DD}} \boldsymbol{\Gamma}_{MN}, \tag{23}$$

where $\boldsymbol{\Gamma}_{MN}$ is a $MN \times MN$ shuffling matrix, and it is obtained by shuffling the columns of the $MN \times MN$ identity matrix. The structure of $\boldsymbol{\Gamma}_{MN}$ can be expressed as follows

$$\boldsymbol{\Gamma}_{MN} = [\boldsymbol{\Gamma}_0, \boldsymbol{\Gamma}_1 \cdots, \boldsymbol{\Gamma}_{M-1}], \tag{24}$$

where $\boldsymbol{\Gamma}_m$, for $m = 0, \cdots, M-1$, is an $MN \times N$ matrix defined as

$$\boldsymbol{\Gamma}_m = [\mathbf{I}_m, \mathbf{I}_{m+N}, \cdots, \mathbf{I}_{m+(N-1)N}] \tag{25}$$

with $\mathbf{I}_m$ being the m-th column of the $MN \times MN$ identity matrix.

The shuffled DD domain channel matrix, $\tilde{\mathbf{H}}^{\text{DD}}$, is obtained by extracting and grouping the elements of $\mathbf{H}^{\text{DD}}$ on the rows and columns with indices $m, m+M, \cdots, m+(N-1)M$ together. The matrix $\tilde{\mathbf{H}}^{\text{DD}}$ can be expressed as a block matrix as

$$\tilde{\mathbf{H}}^{\text{DD}} = \begin{bmatrix} \tilde{\mathbf{H}}_{00}^{\text{DD}} & \tilde{\mathbf{H}}_{01}^{\text{DD}} & \cdots & \tilde{\mathbf{H}}_{0(M-1)}^{\text{DD}} \\ \tilde{\mathbf{H}}_{10}^{\text{DD}} & \tilde{\mathbf{H}}_{11}^{\text{DD}} & \cdots & \tilde{\mathbf{H}}_{1(M-1)}^{\text{DD}} \\ \vdots & \vdots & \cdots & \vdots \\ \tilde{\mathbf{H}}_{(M-1)0}^{\text{DD}} & \tilde{\mathbf{H}}_{(M-1)1}^{\text{DD}} & \cdots & \tilde{\mathbf{H}}_{(M-1)(M-1)}^{\text{DD}} \end{bmatrix}. \tag{26}$$

The sub-matrix, $\tilde{\mathbf{H}}_{kl}^{\text{DD}}$, is an $N \times N$ matrix, with the $(m+1, n+1)$-th element being $h_{kN+m}^{\text{DD}}(lN+n)$, where $h_k^{\text{DD}}(l)$ is the $(k+1, l+1)$-th element of $\mathbf{H}^{\text{DD}}$. We have the following proposition regarding the structure of $\tilde{\mathbf{H}}^{\text{DD}}$.

Proposition III.1. *Assume the number of subcarriers is no less than the length of the equivalent time domain CIR, that is, $M > L$. For the shuffled DD domain channel matrix as shown in* (27)*, the $M \times M$ sub-matrix $\tilde{\mathbf{H}}_{uv}^{DD}$ is an all-zero matrix if $v \neq (u-l)_M$, for all $u = 0, \cdots, M-1$ and $l = 0, \cdots, L$. That is, the shuffled DD domain channel matrix $\tilde{\mathbf{H}}^{DD}$ has a block-circulant-like structure as shown in* (27) *at the top of the next page.*

In order to prove the structure of the shuffled DD domain channel matrix $\tilde{\mathbf{H}}^{\text{DD}}$ as in Proposition III.1, we first need to establish the results in the following Lemma.

Lemma III.1. *Assume $M > L$. Consider $0 \leq v \leq M-1$. If*

$$v \neq (u-l)_M, \tag{28}$$

$$\mathbf{H} = \begin{bmatrix} h_0[0] & 0 & 0 & \cdots & 0 & h_0[L] & \cdots & \cdots & h_0[1] \\ h_1[1] & h_1[0] & 0 & \cdots & 0 & 0 & h_1[L] & \cdots & h_1[2] \\ \vdots & \ddots & \ddots & \ddots & \ddots & \ddots & \ddots & \ddots & \vdots \\ h_L[L] & \cdots & h_L[0] & 0 & \cdots & \cdots & \cdots & \cdots & 0 \\ 0 & h_{L+1}[L] & \cdots & h_{L+1}[0] & 0 & \cdots & \cdots & \cdots & 0 \\ \vdots & \ddots & \ddots & \ddots & \ddots & \ddots & \ddots & \ddots & \vdots \\ 0 & \cdots & \cdots & \cdots & \cdots & 0 & h_{(N-1)(M-1)}[L] & \cdots & h_{(N-1)(M-1)}[0] \end{bmatrix}. \quad (16)$$

$$\tilde{\mathbf{H}}^{\text{DD}} = \begin{bmatrix} \tilde{\mathbf{H}}^{\text{DD}}_{00} & \mathbf{0}_N & \mathbf{0}_N & \cdots & \mathbf{0}_N & \tilde{\mathbf{H}}^{\text{DD}}_{0(M-L)} & \cdots & \cdots & \tilde{\mathbf{H}}^{\text{DD}}_{0(M-1)} \\ \tilde{\mathbf{H}}^{\text{DD}}_{10} & \tilde{\mathbf{H}}^{\text{DD}}_{11} & \mathbf{0}_N & \cdots & \mathbf{0}_N & \mathbf{0}_N & \tilde{\mathbf{H}}^{\text{DD}}_{1(M-L+1)} & \cdots & \tilde{\mathbf{H}}^{\text{DD}}_{1(M-1)} \\ \vdots & \ddots & \ddots & \ddots & \ddots & \ddots & \ddots & \ddots & \vdots \\ \tilde{\mathbf{H}}^{\text{DD}}_{L0} & \cdots & \tilde{\mathbf{H}}^{\text{DD}}_{LL} & \mathbf{0}_N & \cdots & \cdots & \cdots & \cdots & \mathbf{0}_N \\ \mathbf{0}_N & \tilde{\mathbf{H}}^{\text{DD}}_{(L+1)1} & \cdots & \tilde{\mathbf{H}}^{\text{DD}}_{(L+1)(L+1)} & \mathbf{0}_N & \cdots & \cdots & \cdots & \mathbf{0}_N \\ \vdots & \ddots & \ddots & \ddots & \ddots & \ddots & \ddots & \ddots & \vdots \\ \mathbf{0}_N & \cdots & \cdots & \cdots & \mathbf{0}_N & \tilde{\mathbf{H}}^{\text{DD}}_{(M-1)(M-L-1)} & \cdots & \cdots & \tilde{\mathbf{H}}^{\text{DD}}_{(M-1)(M-1)} \end{bmatrix}. \quad (27)$$

for all $u = 0, \cdots, M-1$ *and* $l = 0, \cdots, L$, *then*

$$v + pM \neq (u + qM - l')_{MN}, \quad (29)$$

for all $p, q = 0, \cdots, N-1$ *and* $l' = 0, \cdots, L$.

Proof. Given the range of u, l', and q, we have

$$-M < -L \leq u + qM - l' \leq NM - 1. \quad (30)$$

Thus we have

$$(u + qM - l')_{MN} = u + qM - l' + \tilde{N}M, \quad (31)$$

where $\tilde{N} = N$ if $u + qM - l' < 0$ and $\tilde{N} = N$ otherwise.

From (29) and (31), it is equivalent to prove that $v + pM \neq u + qM - l' + \tilde{N}M$, or

$$v \neq u - l' + (\tilde{N} + q - p)M. \quad (32)$$

We will prove (32) by considering two cases based on the range of $u - l'$. Given the range of u and l', we have

$$-M < -L \leq u - l' \leq M - 1. \quad (33)$$

The two cases are $u - l' \in (-M, 0)$ and $u - l' \in [0, M-1]$.

a) $u - l' \in (-M, 0)$.

When $\tilde{N} + q - p \neq 1$, it is straightforward that (32) is true given that $u - l' + (\tilde{N} + q - p)M \notin [0, M-1]$ and $v \in [0, M-1]$.

When $\tilde{N} + q - p = 1$, we will prove (32) by contradiction. Assume there exists l' such that $v = u - l' + M$, then $v = (u - l')_M$ given that $u - l' \in (-M, 0)$, and this contradicts with (28). Thus (32) holds.

b) $u - l' \in [0, M-1]$.

When $\tilde{N} + q - p \neq 0$, it is straightforward that (32) is true given that $u - l' + (\tilde{N} + q - p)M \notin [0, M-1]$ and $v \in [0, M-1]$.

When $\tilde{N} + q - p = 0$, we will prove (32) by contradiction. Assume there exists l' such that $v = u - l'$, then $v = (u - l')_M$ given that $u - l' \in [0, M-1]$, and this contradicts with (28). Thus (32) holds.

■

Now we are ready to prove the the structure of the shuffled DD domain channel matrix $\tilde{\mathbf{H}}^{\text{DD}}$.

Proof of Proposition III.1. The time domain channel matrix $\mathbf{H}$ in (16) can be represented as an $N \times N$ block matrix as

$$\mathbf{H} = \begin{bmatrix} \mathbf{H}_{00} & \mathbf{H}_{01} & \cdots & \mathbf{H}_{0(N-1)} \\ \mathbf{H}_{10} & \mathbf{H}_{11} & \cdots & \mathbf{H}_{1(N-1)} \\ \vdots & \vdots & \cdots & \vdots \\ \mathbf{H}_{(N-1)0} & \mathbf{H}_{(N-1)1} & \cdots & \mathbf{H}_{(N-1)(N-1)} \end{bmatrix}, \quad (34)$$

where the $(m+1, n+1)$-th element of the $(k+1, l+1)$-th block, $\mathbf{H}_{kl} \in \mathcal{C}^{M \times M}$, is $h_{kM+m}(lM+n)$, for $m, n = 0, \cdots, M-1$ and $k, l = 0, \cdots, N-1$. It should be noted that a large number of elements in $\mathbf{H}_{kl}$ will be 0 due to the finite channel length as shown in (16).

From (22) and (34), $\mathbf{H}^{\text{DD}}$ can be written as an $N \times N$ block matrix with the (m, n)-th block being

$$\mathbf{H}^{\text{DD}}_{mn} = \sum_{k=0}^{N-1} \sum_{l=0}^{N-1} e^{-j2\pi \frac{mk}{N}} \cdot \mathbf{H}_{kl} \cdot e^{j2\pi \frac{nl}{N}} \in \mathcal{C}^{M \times M}. \quad (35)$$

If we extract the (u, v)-th elements of $\mathbf{H}^{\text{DD}}_{mn}$, for all $m, n = 0, \cdots, N-1$, and then use them to form an $N \times N$ matrix, we have

$$\tilde{\mathbf{H}}^{\text{DD}}_{uv} = \mathbf{F}_N \cdot \tilde{\mathbf{H}}_{uv} \cdot \mathbf{F}_N^H \in \mathcal{C}^{N \times N}, \quad (36)$$

where $\tilde{\mathbf{H}}_{uv}$ is an $N \times N$ matrix made up by the (u, v)-th elements of $\mathbf{H}_{mn}$, that is, the (m, n)-th element of $\tilde{\mathbf{H}}_{uv}$ is the (u, v)-th element of $\mathbf{H}_{mn}$.

From (16), the $(p+1, q+1)$-th element in $\tilde{\mathbf{H}}_{uv}$ can be represented as $h_{u+pM}[v + qN]$, for $p, q = 0, \cdots, N-1$. From Lemma III.1, it has been shown that if $v \neq (u - l)_M$, then the

indices of all elements in $\tilde{\mathbf{H}}_{uv}$ satisfy $v+pM \neq (u+qM-l')_{MN}$, for $p,q=0,\cdots,N-1$ and $l'=0,\cdots,L$. From (16), we have $h_u[v]=0$ if $v \neq u,(u-1)_{NM},\cdots$, or $(u-L)_{NM}$.

Combining the above facts, we have that all elements in $\tilde{\mathbf{H}}_{uv}$ are 0 if $v \neq (u-l)_M$. Consequently, from (36), $\tilde{\mathbf{H}}^{\text{DD}}_{uv}$ is an all-zero matrix if $v \neq (u-l)_M$. This completes the proof. ■

With the shuffled DD domain channel matrix and the fact that $\mathbf{\Gamma}^T_{MN}\mathbf{\Gamma}_{MN}=\mathbf{I}_{MN}$, the DD domain system equation in (20) can be alternatively written as

$$\tilde{\mathbf{y}}^{\text{DD}} = \tilde{\mathbf{H}}^{\text{DD}}\tilde{\mathbf{x}}^{\text{DD}} + \tilde{\mathbf{z}}^{\text{DD}}, \tag{37}$$

where

$$\tilde{\mathbf{y}}^{\text{DD}} = \mathbf{\Gamma}^T_{MN}\text{vec}\left(\mathbf{Y}^{\text{DD}}\right) = \left[\left(\tilde{\mathbf{y}}^{\text{DD}}_1\right)^T,\cdots,\left(\tilde{\mathbf{y}}^{\text{DD}}_M\right)^T\right]^T, \tag{38}$$

$$\tilde{\mathbf{x}}^{\text{DD}} = \mathbf{\Gamma}^T_{MN}\text{vec}\left(\mathbf{X}^{\text{DD}}\right) = \left[\left(\tilde{\mathbf{x}}^{\text{DD}}_1\right)^T,\cdots,\left(\tilde{\mathbf{x}}^{\text{DD}}_M\right)^T\right]^T, \tag{39}$$

$$\tilde{\mathbf{z}}^{\text{DD}} = \mathbf{\Gamma}^T_{MN}\text{vec}\left(\mathbf{Z}^{\text{DD}}\right) = \left[\left(\tilde{\mathbf{z}}^{\text{DD}}_1\right)^T,\cdots,\left(\tilde{\mathbf{z}}^{\text{DD}}_M\right)^T\right]^T, \tag{40}$$

where $\tilde{\mathbf{y}}^{\text{DD}}_m$, $\tilde{\mathbf{x}}^{\text{DD}}_m$, and $\tilde{\mathbf{z}}^{\text{DD}}_m$ are length-N sub-vectors of $\tilde{\mathbf{y}}^{\text{DD}}$, $\tilde{\mathbf{x}}^{\text{DD}}$, and $\tilde{\mathbf{z}}^{\text{DD}}$, respectively, for $m=1,\cdots,M$.

IV. Receiver Design

We propose to design a new low complexity receiver based on the special structure of the shuffled DD domain matrix as presented in Proposition III.1.

With the system equation given in (20), the optimum maximum likelihood (ML) receiver can be designed as

$$\widehat{\tilde{\mathbf{x}}^{\text{DD}}} = \underset{\tilde{\mathbf{x}}^{\text{DD}}\in\mathcal{M}^{NM\times 1}}{\arg\min}\left[(\tilde{\mathbf{y}}^{\text{DD}}-\tilde{\mathbf{H}}^{\text{DD}}\tilde{\mathbf{x}}^{\text{DD}})^H(\tilde{\mathbf{y}}^{\text{DD}}-\tilde{\mathbf{H}}^{\text{DD}}\tilde{\mathbf{x}}^{\text{DD}})\right], \tag{41}$$

where $\mathcal{M}$ is the set of modulation symbols. The complexity of the ML receiver grows exponentially with the modulation level and the size of N and M, and it becomes prohibitively high for larger values of N and M.

We propose to develop an iterative receiver to exploit the block-circulant-like structure of the DD domain channel matrix $\tilde{\mathbf{H}}^{\text{DD}}$ as shown in (27). The proposed receiver employes successive interference cancellation. Assume the previously detected symbols as $\hat{\mathbf{x}}^{\text{DD}}_n$, and define the difference between $\tilde{\mathbf{x}}^{\text{DD}}_n$ and $\hat{\mathbf{x}}^{\text{DD}}_n$ as $\mathbf{e}^{\text{DD}}_n = \tilde{\mathbf{x}}^{\text{DD}}_n - \hat{\mathbf{x}}^{\text{DD}}_n$.

From (27) and (37), the received signals corresponding to the n-th DD domain data block, $\tilde{\mathbf{x}}^{\text{DD}}_n$, is

$$\tilde{\mathbf{y}}^{\text{DD}}_{n+l} = \tilde{\mathbf{H}}^{\text{DD}}_{(n+l)n}\tilde{\mathbf{x}}^{\text{DD}}_n + \sum_{\substack{k=0\\k\neq l}}^{L}\tilde{\mathbf{H}}^{\text{DD}}_{(n+l)(n+l-k)_M}\tilde{\mathbf{x}}^{\text{DD}}_{(n+l-k)_M} + \tilde{\mathbf{z}}^{\text{DD}}_{n+l},$$
$$\text{for } l=0,\cdots,L. \tag{42}$$

The system model in (42) is used to detect $\tilde{\mathbf{x}}^{\text{DD}}_n$, and $\left\{\tilde{\mathbf{x}}^{\text{DD}}_{(n+l-k)_N}\right\}_{k=0,k\neq l}^{L}$ are treated as interference. Applying interference cancellation to (42) by using the previously symbols yields

$$\begin{aligned}\check{\mathbf{y}}^{\text{DD}}_{n+l} &= \tilde{\mathbf{y}}^{\text{DD}}_{n+l} - \sum_{\substack{k=0\\k\neq l}}^{L}\tilde{\mathbf{H}}^{\text{DD}}_{(n+l)_M(n+l-k)_M}\hat{\mathbf{x}}^{\text{DD}}_{(n+l-k)_M},\\ &= \tilde{\mathbf{H}}^{\text{DD}}_{(n+l)_M n}\tilde{\mathbf{x}}^{\text{DD}}_n + \tilde{\mathbf{z}}^{\text{DD}}_{(n+l)_M},\ \text{for } l=0,\cdots,L,\end{aligned} \tag{43}$$

where the second equality is based on the assumption of perfect interference cancellation.

Performing coherent matrix combining (CMC) over $\left\{\check{\mathbf{y}}^{\text{DD}}_{n+l}\right\}_{l=0}^{L}$ as

$$\boldsymbol{\gamma}_n = \sum_{l=0}^{L}\left(\tilde{\mathbf{H}}^{\text{DD}}_{(n+l)n}\right)^H\check{\mathbf{y}}^{\text{DD}}_{n+l}. \tag{44}$$

The DD domain system equation in (43) after CMC can be expressed as

$$\boldsymbol{\gamma}_n = \mathbf{\Lambda}_n\tilde{\mathbf{x}}^{\text{DD}}_n + \boldsymbol{\varepsilon}_n, \tag{45}$$

where

$$\begin{aligned}\mathbf{\Lambda}_n &= \sum_{l=0}^{L}\left(\tilde{\mathbf{H}}^{\text{DD}}_{(n+l)n}\right)^H\tilde{\mathbf{H}}^{\text{DD}}_{(n+l)n},\\ \boldsymbol{\varepsilon}_n &= \sum_{l=0}^{L}\left(\tilde{\mathbf{H}}^{\text{DD}}_{(n+l)n}\right)^H\tilde{\mathbf{z}}^{\text{DD}}_{n+l}.\end{aligned} \tag{46}$$

We propose to detect $\tilde{\mathbf{x}}^{\text{DD}}_n$ from $\boldsymbol{\gamma}_n$ by following the MMSE criterion as $\hat{\mathbf{x}}^{\text{DD}}_n = \mathbf{W}_n\boldsymbol{\gamma}_n$, where $\mathbf{W}_n$ is the MMSE matrix. The soft output of MMSE, $\hat{\mathbf{x}}^{\text{DD}}_n$, is first hard detected to the modulation constellation as $\tilde{\mathbf{x}}^{\text{DD}}_n$, which are then used during interference cancellation for subsequent detections. The MMSE matrix can be calculated by following the orthogonality principle

$$\mathbb{E}[(\mathbf{W}_n\boldsymbol{\gamma}_n - \hat{\mathbf{x}}^{\text{DD}}_n)\boldsymbol{\gamma}^H_n] = \mathbf{0}. \tag{47}$$

Solving (47) yields

$$\mathbf{W}_n = \mathbf{\Lambda}^H_n\left(\mathbf{\Lambda}_n\mathbf{\Lambda}^H_n + \frac{N_0}{E_s}\mathbf{\Lambda}_n\right)^{-1}. \tag{48}$$

In the proposed iterative algorithm, in each iteration, the data in the n-th DD domain data block, $\tilde{\mathbf{x}}^{\text{DD}}_n$, is detected by first performing interference cancellation as in (43), then CMC as in (44), and finally MMSE detection. The detected symbols, $\{\hat{\mathbf{x}}^{\text{DD}}_n\}_{n=1}^{N}$, are hard detected to the modulation constellation, then used during interference cancellation for the subsequent symbols. The inputs to the first iteration are assumed to be 0. The iteration terminates when the output of two consecutive iterations are the same, or the maximum number of iterations is reached.

V. Simulation Results

The performance of the proposed low complexity detector is evaluated in this section. The carrier frequency is set at 4 GHz. The subcarrier spacing Δf is set at 15 KHz. The physical channel is generated with an EVA delay profile [12] under various speeds of the user equipment (UE). In all simulations, the maximum iterations of the DD-MMSE and MP receivers are set at 8 and 40, respectively.

Figure 1 compares the performance of the proposed CMC-MMSE receiver with the MP receiver [6]. The UE speed is set at 500 km/hr, which corresponds to a maximum Doppler spread f_{D} = 1,852 Hz. The value of M is fixed at 64, under various values of N. When N = 16, 32, 64, the normalized Doppler spreads, $f_{\text{D}}NT$, are 1.98, 3.95, and 7.90, respectively,

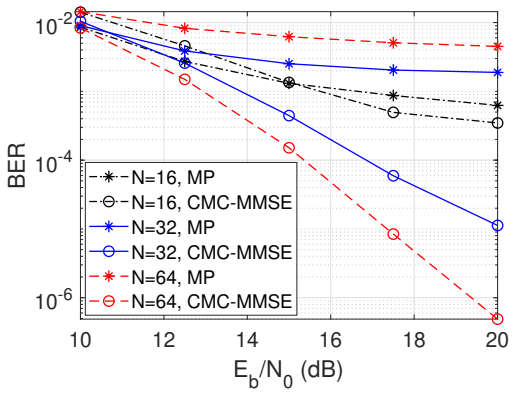

Fig. 1: Comparison between CMC-MMSE and MP under $M = 64$ and different N values (UE speed 500 km/hr).

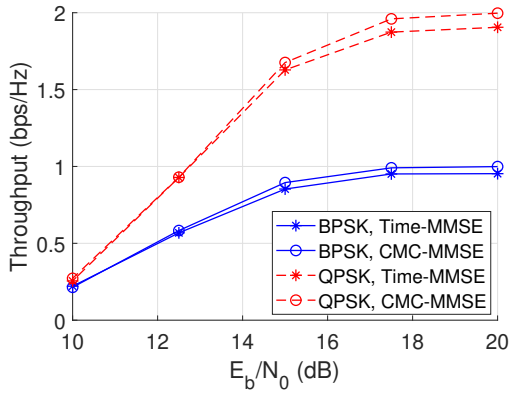

Fig. 2: Throughput of CMC-MMSE in OTFS and Time-MMSE in ZP-OTFS [5] ($M = N = 64$, UE speed 500 km/hr)

which correspond to increase in Doppler diversity [13]. During simulations, the CMC-MMSE algorithm converges usually within 3 iterations. As expected, the performance of the OTFS system with the proposed CMC-MMSE receiver consistently improves as N becomes larger, and they significantly outperform their MP counterparts under all system configurations. The performance different is more pronounced at larger N. For systems with MP receiver, error floors are observed at high E_b/N_0 due to the limit of the receiver.

Figure 2 compares the throughput of the proposed CMC-MMSE with the time-domain MMSE (time-MMSE) algorithm [5]. The time-MMSE algorithm has to be used for ZP-OTFS yet the CMC-MMSE is tested with regular OTFS. The throughput is calculated as $\frac{\log_2|\mathcal{M}|K}{NTM\Delta f}(1-\texttt{FER})$, where K is the total number of symbols for each frame, FER is the frame error rate (FER), and $\mathcal{M}$ is the modulation constellation. For regular OTFS, we have $K = NM$, and the value of K is $N(M-L)$ due to the padding of NL zeros at the end of the ZP-OTFS frame. CMC-MMSE and time-MMSE have similar BER performance and complexity. However, CMC-MMSE slightly outperforms time-MMSE in terms of throughput due to the lower spectral efficiency of ZP-OTFS required by time-MMSE.

VI. Conclusions

We have designed a new low complexity CMC-MMSE receiver for OTFS systems. The receiver was designed by exploiting the block-circulant-like structure of the DD domain channel matrix. The DD domain channel matrix structure was enabled by shuffling the DD domain received samples such that samples experiencing the same delays but with different Doppler spreads are grouped together. CMC and MMSE was utilized to collect the diversity and mitigate the interference in the delay and Doppler domains, respectively. Simulation results have demonstrated that the proposed CMC-MMSE receiver can achieve simultaneous diversity collection and interference suppression in both the delay and Doppler domains, and it achieves significant performance gains over the commonly used MP receivers.

References

[1] R. Hadani, S. Rakib, M. Tsatsanis, A. Monk, A. J. Goldsmith, A. F. Molisch, and R. Calderbank, "Orthogonal time frequency space modulation," in *2017 IEEE Wireless Communications and Networking Conference (WCNC)*. IEEE, 2017, pp. 1–6.

[2] R. Hadani and A. Monk, "OTFS: A new generation of modulation addressing the challenges of 5G," *arXiv preprint arXiv:1802.02623*, 2018.

[3] L. Gaudio, G. Colavolpe, and G. Caire, "OTFS vs. OFDM in the presence of sparsity: A fair comparison," *IEEE Transactions on Wireless Communications*, vol. 21, no. 6, pp. 4410–4423, 2021.

[4] T. Zemen, M. Hofer, and D. Loeschenbrand, "Low-complexity equalization for orthogonal time and frequency signaling (OTFS)," *arXiv preprint arXiv:1710.09916*, 2017.

[5] Q. Li, J. Yuan, and H. Lin, "Iterative mmse detection for orthogonal time frequency space modulation," in *2022 IEEE International Conference on Communications Workshops (ICC Workshops)*. IEEE, 2022, pp. 01–06.

[6] P. Raviteja, K. T. Phan, Y. Hong, and E. Viterbo, "Interference cancellation and iterative detection for orthogonal time frequency space modulation," *IEEE transactions on wireless communications*, vol. 17, no. 10, pp. 6501–6515, 2018.

[7] Z. Yuan, F. Liu, W. Yuan, Q. Guo, Z. Wang, and J. Yuan, "Iterative detection for orthogonal time frequency space modulation with unitary approximate message passing," *IEEE transactions on wireless communications*, vol. 21, no. 2, pp. 714–725, 2021.

[8] T. Thaj and E. Viterbo, "Low complexity iterative rake detector for orthogonal time frequency space modulation," in *2020 IEEE Wireless Communications and Networking Conference (WCNC)*. IEEE, 2020, pp. 1–6.

[9] S. Li, W. Yuan, Z. Wei, and J. Yuan, "Cross domain iterative detection for orthogonal time frequency space modulation," *IEEE transactions on wireless communications*, vol. 21, no. 4, pp. 2227–2242, 2021.

[10] A. Zhou, Y. Pan, J. Wu, H. Lin, and J. Yuan, "On the performance of practical pulse-shaped OTFS with analog receivers," in *IEEE ICC 2023 Workshop on OTFS and Delay-Doppler Multicarrier Communications for 6G*. IEEE, 2023, pp. 1–6.

[11] K. B. Petersen, M. S. Pedersen *et al.*, "The matrix cookbook," *Technical University of Denmark*, vol. 7, no. 15, p. 510, 2008.

[12] ETSI LTE, "Evolved universal terrestrial radio access (E-UTRA); base station (BS) radio transmission and reception (3GPP TS 36.104 version 8.6. 0 release 8), july 2009," *ETSI TS*, vol. 136, no. 104, p. V8, 2009.

[13] W. Zhou, J. Wu, and P. Fan, "High mobility wireless communications with doppler diversity: Fundamental performance limits," *IEEE Transactions on Wireless communications*, vol. 14, no. 12, pp. 6981–6992, 2015.